

# Experimental and Numerical Study of High Froude-number Resistance of Ship Utilizing a Hull Vane<sup>®</sup>: A Case Study of a Hard-chine Crew Boat


 Open  
Access

 Soegeng Riyadi<sup>1,2</sup>, Ketut Suastika<sup>1,\*</sup>
<sup>1</sup> Department of Naval Architecture, Faculty of Marine Technology, Institut Teknologi Sepuluh Nopember (ITS), Surabaya 60111, Indonesia

<sup>2</sup> PT. Orela Shipyard, Gresik 61154, Indonesia

## ARTICLE INFO

### Article history:

Received 22 December 2019

Received in revised form 18 February 2020

Accepted 23 February 2020

Available online 29 February 2020

### Keywords:

CFD; hard-chine crew boat; high Froude-number range; ship resistance; towing-tank experiments

## ABSTRACT

Energy efficiency and environmental sustainability are key performance indicators in the development of services and products nowadays. This study is motivated by the inquiry whether a lower ship resistance, thus energy efficiency due to saving of fuel consumption, is achievable if a Hull Vane<sup>®</sup> is to be retrofitted into a high-speed vessel at  $Fr > 0.6$ . Experimental and numerical studies were performed, utilizing a hard-chine crew boat with varying vane's placement in the longitudinal direction. At  $Fr > 0.75$  all vane's placement variations resulted in an increase of total ship resistance, reaching a value of 36.3% at  $Fr = 0.92$  for the vane's placement with the leading edge one chord length behind the transom. A bow-down trim was observed in this high Froude-number range, which became more pronounced with increasing  $Fr$ . The vane's placement with the leading edge two chord lengths behind the transom was found to be the most favourable vane's placement among the variations considered, which resulted in a decrease of ship resistance at  $Fr < 0.74$ , reaching a value of 7.1% at  $Fr = 0.62$ .

Copyright © 2020 PENERBIT AKADEMIA BARU - All rights reserved

## 1. Introduction

Energy efficiency and environmental sustainability are mandatory requirements in the design, development and operation of ships nowadays. For example, the energy efficiency design index (EEDI) is mandatory for new ships and the ship energy efficiency management plan (SEEMP) is required for all ships [1-2]. The research area considering fuel efficiency of ships can be divided into four main themes: engine and propulsion efficiencies, alternative renewable resources and ship resistance reduction [3]. Regarding the ship resistance reduction, which is the focus of this study, many innovations have been made, among others those utilizing appendages. The most successful application is the so-called Hull Vane<sup>®</sup>, invented by van Oossanen in 1992 and patented in 2002.

When applied to a ship, the Hull Vane<sup>®</sup> can generate an additional thrust, thereby reducing the bow-up trim and reducing the generation of waves. Furthermore, it can reduce the vessel's motions

\* Corresponding author.

E-mail address: [k\\_suastika@na.its.ac.id](mailto:k_suastika@na.its.ac.id) (Ketut Suastika)

in waves, leading to a higher comfort level for the crew and passengers. Successful applications were reported when a Hull Vane<sup>®</sup> was applied to a 108 m Holland-Class OPV. Beside resistance reduction, other benefits include lower vertical acceleration, an increased sailing range and increased top speed [4-5]. Better seakeeping performances were also reported due to Hull Vane<sup>®</sup>'s applications to ferries and ro-pax vessels [6].

Comparing the performances of the Hull Vane<sup>®</sup>, interceptors, trim wedges and ballasting utilizing CFD simulations, the Hull Vane<sup>®</sup> was found to be the most efficient device in reducing the ship resistance and in improving the seakeeping performance [7]. The resistance reduction reached 32.4% in the Froude-number range  $0.2 < Fr < 0.6$  while in the higher Froude-number range ( $0.6 < Fr < 0.8$ ), the resistance reduction was approximately between 10-12%.

The Hull Vane<sup>®</sup> has been applied to different types of vessel, such as sailing yachts, motor yachts, supply vessels, container ships, cruise ships and ro-ro vessels and it was found that in certain applications a resistance increase was found. Bulk carriers and crude oil carriers are not suitable for Hull Vane<sup>®</sup>'s applications but supply vessels, ferries or patrol vessels are.

The Hull Vane<sup>®</sup> should not be placed too close to the hull and not too far below the hull as the angle of attack from the water would result in poorer lift generation and less net forward thrust. It should be placed aft of the transom and not too close to the free surface [3, 8-9]. Considering the vane's position in the longitudinal direction, the position with the leading edge two chord lengths behind the transom was found to be the most favorable one [10]. The same object study was considered in Ref. [10] as in this study but their focus was on the lower Froude-number range ( $0.3 < Fr < 0.8$ ).

Each case must be considered separately when a Hull Vane<sup>®</sup> is to be retrofitted into an existing vessel. This process is rather time consuming. A guideline regarding the type of vane's section, its size and its position relative to the ship's hull both in the vertical and longitudinal directions will be very valuable. Furthermore, relatively little information is available for Hull Vane<sup>®</sup>'s applications in the higher Froude-number range ( $0.6 < Fr < 1.0$ ) and the available experimental data in this Froude-number range are scarce. So, the focus of this study is on the Hull Vane<sup>®</sup>'s applications at  $Fr > 0.6$  with varying vane's position in the longitudinal direction. The inquiry whether a lower ship resistance, thus energy efficiency due to saving of fuel consumption, is achievable in this high Froude-number range takes a central role.

## 2. Methodology

CFD simulations were performed with varying Froude numbers in the range  $0.6 < Fr < 1.0$  for ship with and without vane. The vane's section is the NACA 64<sub>1</sub>-212 [9] with aspect ratio of 8.50 (chord  $c = 0.8$  m and span  $s = 6.8$  m) following the results reported in Ref. [10-11]. The vane's position was varied in the longitudinal direction, but its elevation was kept constant at  $h = 0.75 T$  below the water surface, where  $T$  is the boat's draft. Three vane's placement variations were considered as summarized in Table 1. The CFD results were verified using data from towing tank experiments.

As a case study, a hard-chine crew boat was considered, which was designed and produced by PT. Orelia Shipyard, Gresik, Indonesia. Its target top speed is 27 knots ( $Fr = 0.86$ ). The ship particulars are summarized in Table 2.

### 2.1 CFD Simulations

CFD simulations were performed utilizing the software Fine/Marine<sup>®</sup> from Numeca [12]. Figure 1 shows a mesh of the vessel with vane attached to the hull by using two struts for Case 3 (see Table

1). Due to symmetry, only half of the vessel with vane and struts were modeled. A non-uniform mesh distribution was utilized, that is, finer meshes for the vane (NACA 64<sub>1</sub>-212), struts (NACA 0010) and regions of the ship's hull with relatively large curvatures.

**Table 1**

Variation of vane's placement in the longitudinal direction

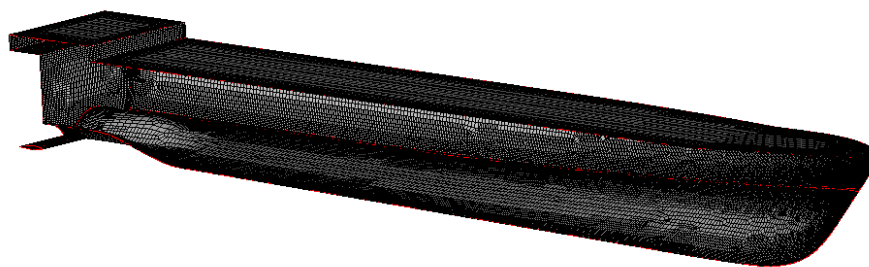
| Case                 | $h/T$ | Position of vane's leading edge    |
|----------------------|-------|------------------------------------|
| Case 0: Without vane | -     | -                                  |
| Case 1               | 0.75  | Precisely below the transom        |
| Case 2               | 0.75  | 1 chord length behind the transom  |
| Case 3               | 0.75  | 2 chord lengths behind the transom |

$h$  = vane's submerged elevation below the water surface  
 $T$  = boat's draft

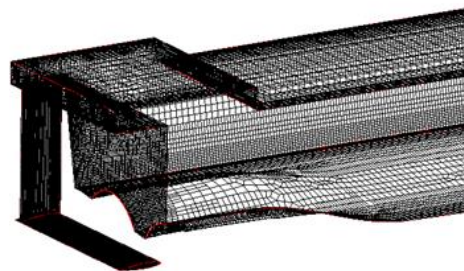
**Table 2**

Ship particulars

| Parameter                                  | Value with unit |
|--|-----------------|
| Length Overall ( $L_{OA}$ )                | 31.20 m         |
| Length Between Perpendiculars ( $L_{BP}$ ) | 28.80 m         |
| Breadth ( $B$ )                            | 6.80 m          |
| Depth ( $H$ )                              | 2.75 m          |
| Draft ( $T$ )                              | 1.40 m          |
| Top Speed ( $V_{max}$ )                    | 27 kn           |
| Displacement ( $\Delta$ )                  | 104.68 t        |



(a)



(b)

**Fig. 1.** (a) Mesh of half of the vessel with vane and struts for Case 3, (b) the stern region zoomed in from (a)

Figure 2 shows a mesh of the computational domain with the vessel inside it for Case 3. The locations of the domain boundaries are defined as follows [13]. The inlet is located at  $1.0 L$  upstream from the vessel, while the outlet is located at  $3.0 L$  behind the vessel. The side wall is located at  $1.50 L$  side the vessel. The bottom wall is located at  $1.50 L$  below the vessel and the top wall is located at

0.50  $L$  above the vessel ( $L$  is the length between the perpendiculars  $L_{BP}$ ). The boundary conditions, resolved motions and convergence criterion are summarized in Table 3.

The turbulence model used is the  $k-\omega$  SST (shear stress transport) model [14]. Free surface effects (generation of waves) were modeled in the simulations [15-16] but effects of shallow water on the ship resistance were not considered (see, for example, in Ref. [17] for shallow water effects on the resistance of high-speed crafts).

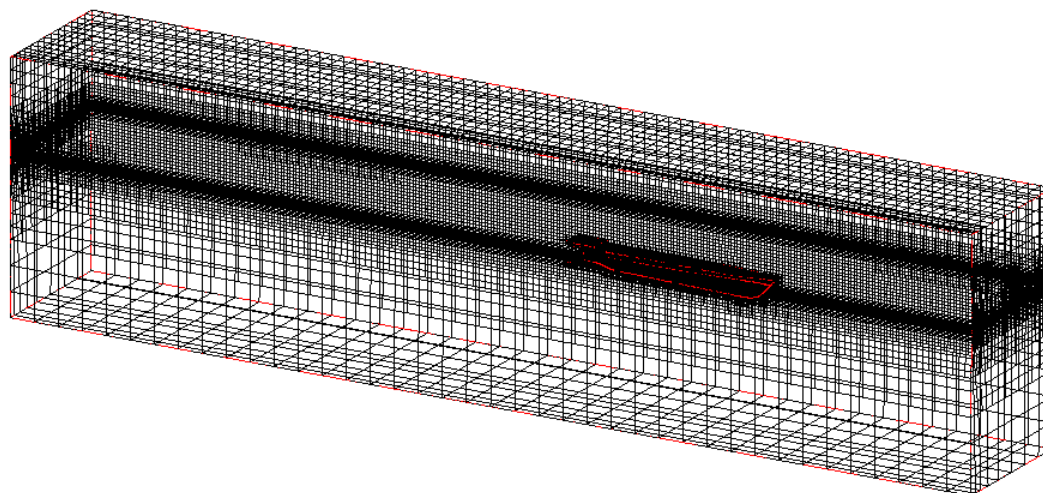


**Fig. 2.** Mesh of the computational domain with the vessel inside it for Case 3

**Table 3**

Boundary conditions, resolved motions and convergence criterion

| Description           | Type  | Condition   |
|-----------------------|---|---|
| Inlet ( $X_{min}$ )   | EXT   | Far field, $V_x = 0$                                  |
| Outlet ( $X_{max}$ )  | EXT   | Far field, $V_x = 0$                                  |
| Bottom ( $Z_{min}$ )  | EXT   | Update hydrostatic pressure                           |
| Top ( $Z_{max}$ )     | EXT   | Update hydrostatic pressure                           |
| Side ( $Y_{min}$ )    | MIR   | Mirror  |
| Side ( $Y_{max}$ )    | EXT   | Far field, $V_x = 0$                                  |
| Ship hull             | SOL   | Wall function   |
| Ship deck             | SOL   | Free slip (zero shear stress)                         |
| Motion                | Translation in X direction<br>with a given speed          | Speed = Ship speed, using<br>one half sinusoidal ramp |
|                       | Translation in Z direction<br>(heave); solved motion type | Linear law  |
|                       | Rotation about the Y axis<br>(pitch); solved motion type  | Linear law  |
| Convergence criterion | Order of magnitude of<br>residual decrease                | Second order  |

In any CFD study, there is a trade-off between accuracy and computational cost. To find an optimum number of cells, grid independence tests were performed. An example is illustrated in Figure 3. A criterion for the fulfillment of the grid independence test is that the relative difference between results (of ship resistances) of two subsequent simulations, with the number of cells in the latter simulation approximately twice of that in the former, must be less than 2% [18]. Using this criterion, the optimum number of cells found for this example was two million and eight hundred thousand.

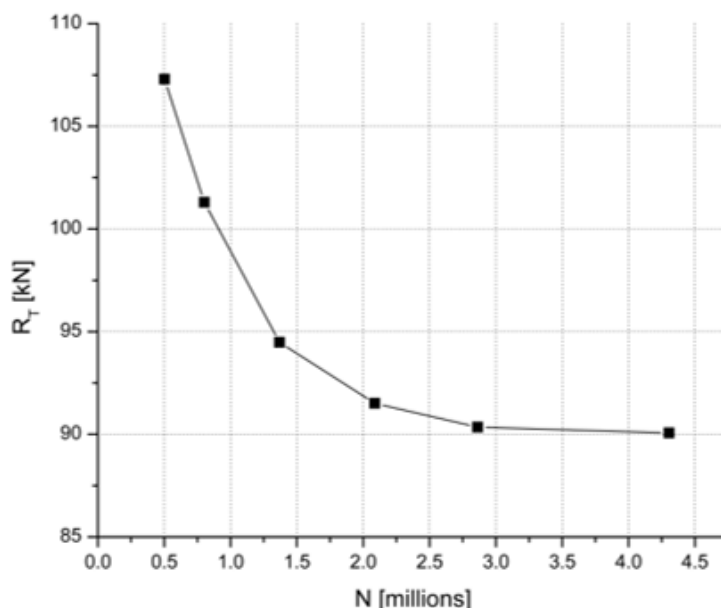


**Fig. 3.** Total ship resistance as function of number of cells used in the simulation ( $Fr = 0.62$ ), illustrating a grid-independence test

## 2.2 Towing-Tank Experiments

The towing-tank experiments were conducted at the Hydrodynamics Laboratory of the Faculty of Marine Technology, ITS Surabaya, Indonesia. The purpose of the towing tests is to verify the results obtained from the CFD simulations. The dimensions of the tank are as follows: length = 50.0 m, width = 3.0 m, and maximum water depth = 2.0 m.

It is necessary to model the vessel in accordance to the size and capacity of the tank. The Froude scaling was applied with a geometrical scale of 1:40. The model consists of a boat’s hull, a vane and two struts. The boat’s model was made from fiberglass-reinforced plastic (FRP) coated with paint and resin. The vane (NACA 64<sub>1</sub>-212) and the struts (NACA 0010) were made from brass. Figure 4 shows the side and aft views of the ship model.

The total resistance of the boat (with or without Hull Vane®) was measured by using a load cell. The load cell was connected to a voltage amplifier, which was connected to a computer network in the control room. The load cell was calibrated by using a mass of 0.5 kg before performing a measurement. The test program is summarized in Table 4 for the Cases 0, 1, 2 and 3. Figure 5 shows the ship model towed at a speed of 1.62 m/s ( $Fr = 0.62$ ) for Case 3.

**Table 4**  
 Test program for the Cases 0, 1, 2 and 3

| $V_{ship}$ [knots] | $V_{model}$ [m/s] | Fr   |
|--------------------|-------------------|------|
| 20                 | 1.62              | 0.62 |
| 22                 | 1.79              | 0.68 |
| 24                 | 1.95              | 0.74 |
| 26                 | 2.12              | 0.80 |
| 28                 | 2.28              | 0.86 |
| 30                 | 2.44              | 0.92 |

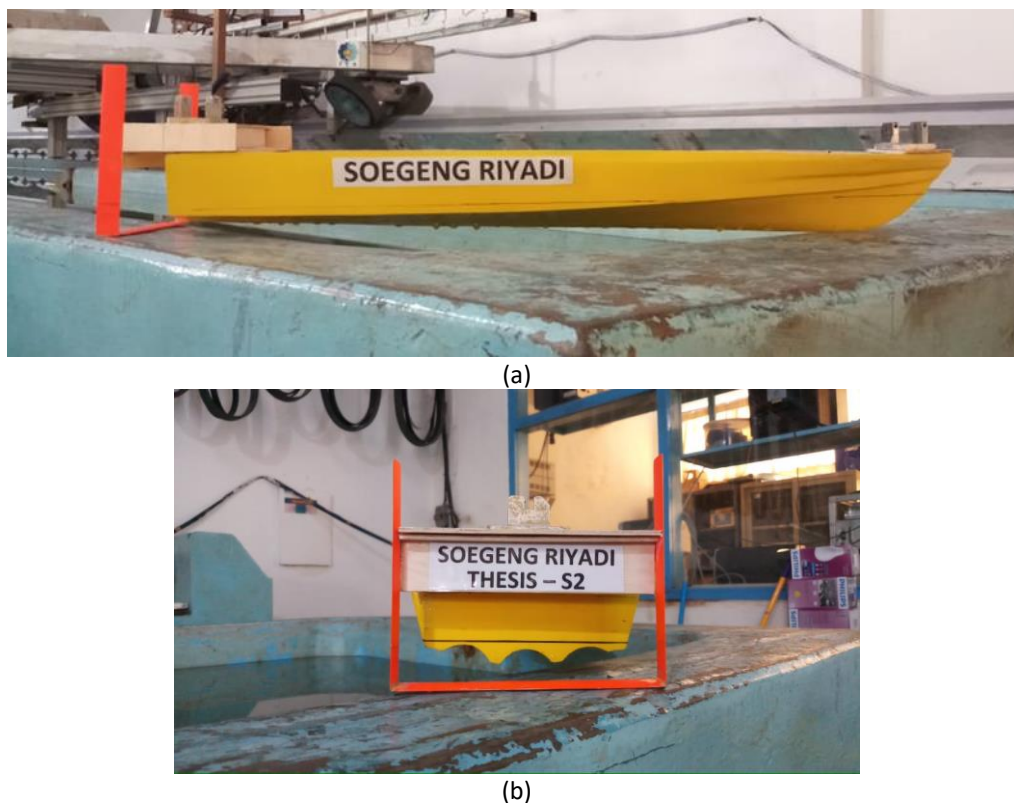


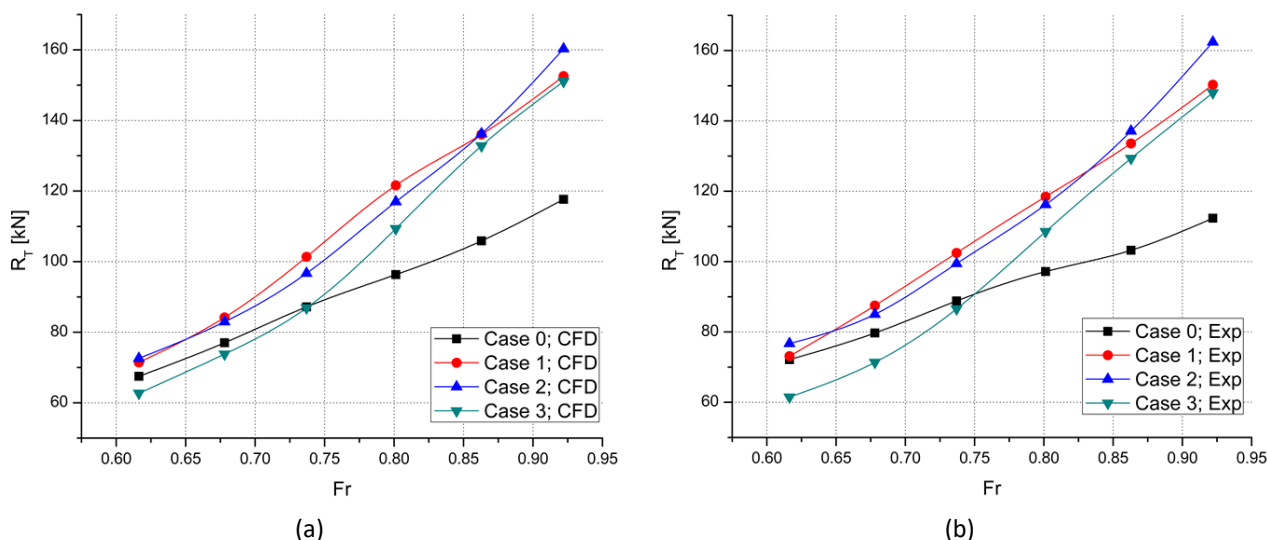
**Fig. 4.** Ship model with a vane attached to the hull by using two struts (scale 1:40): (a) side view and (b) aft view



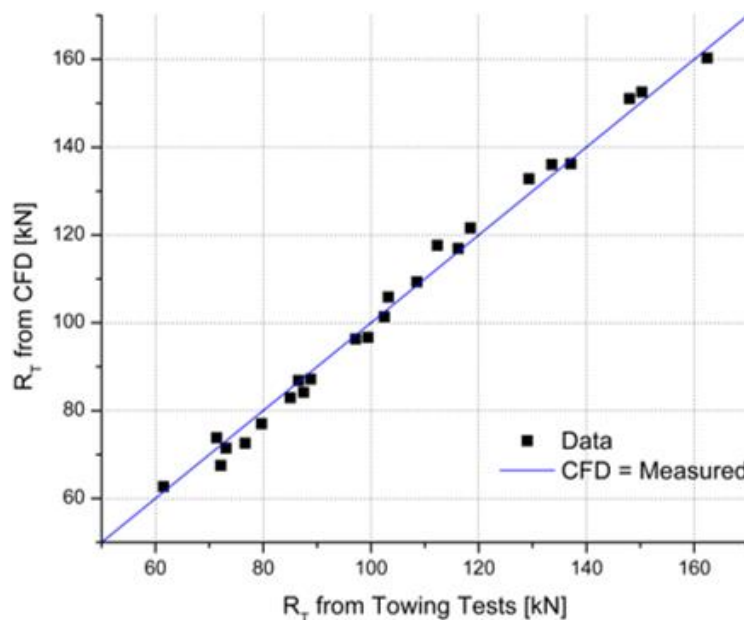
**Fig. 5.** Ship model towed at a speed of 1.62 m/s ( $Fr = 0.62$ ) for Case 3. The locally high water-overflow near the bow is partly ascribed to the hard chine body

### 3. Results and Discussion

Figure 6 shows the total ship resistance as function of the Froude number obtained from the CFD simulations and the towing tests. The agreement between the results from the CFD simulations and the towing tests is good as shown in Figure 7. In the following discussion, the results are compared to the case without vane (Case 0) as a reference case.



**Fig. 6.** Total ship resistance as function of Froude number for ship with and without vane; (a) obtained from the CFD simulations and (b) from the towing tests



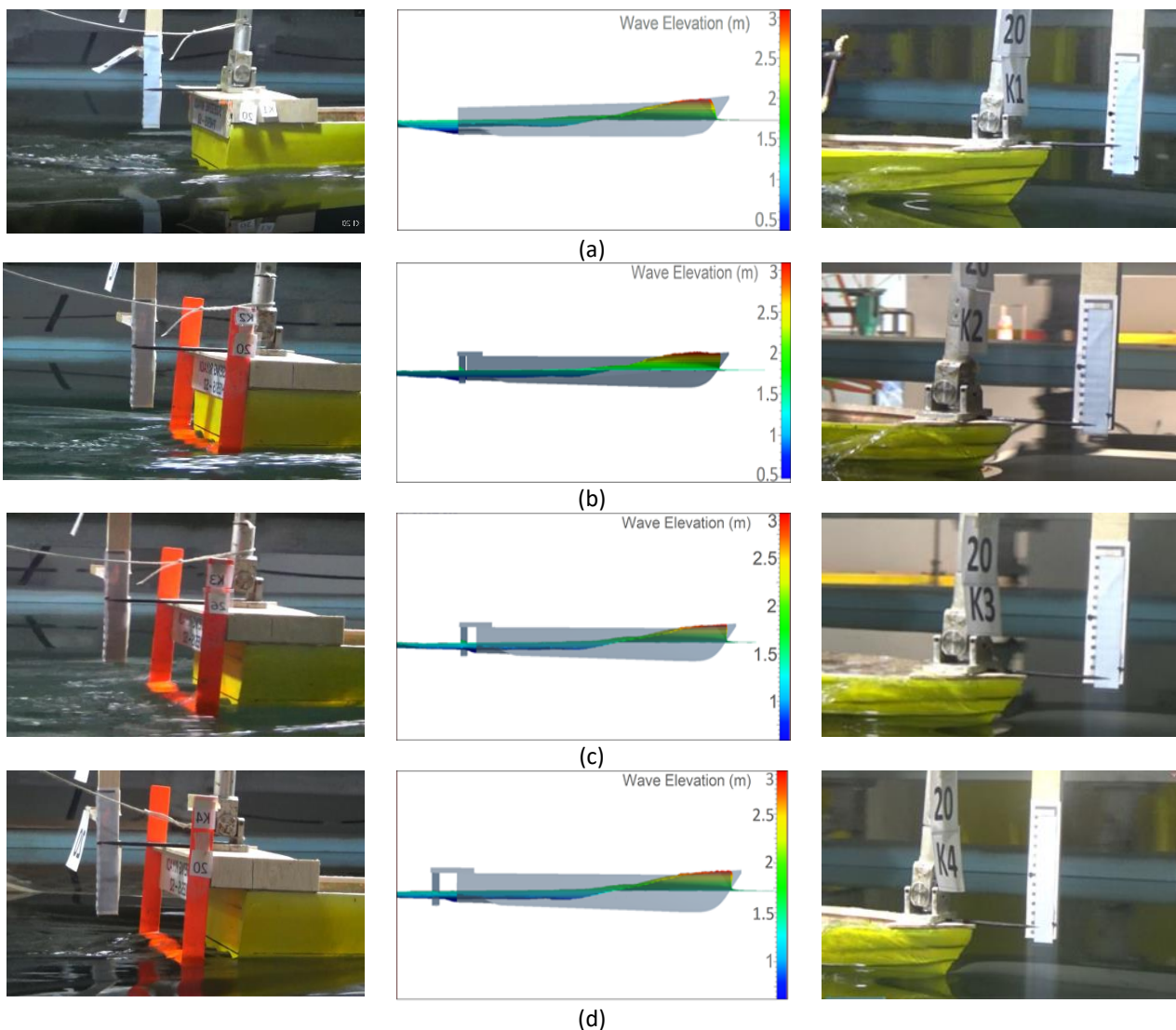
**Fig. 7.** Total ship resistance obtained from the CFD simulations versus that obtained from the towing tests for the Cases 0, 1, 2 and 3

Figure 6 shows that the application of a vane generally results in an increase of total ship-resistance in this high Froude-number range. The increase can reach 36.3% at  $Fr = 0.92$  for Case 2. Furthermore, the vane’s position with the leading edge two chord lengths behind the transom (Case 3) gives the smallest resistance among the vane’s placements considered. Case 3 shows a decrease of ship resistance at  $Fr < 0.74$ . The decrease can reach 7.1% at  $Fr = 0.62$ . At  $Fr > 0.75$  all vane’s placements result in an increase of ship resistance.

The above observations are in a good agreement with those reported in Ref. [3] stating that the Hull Vane® works most favourably at moderate to high Froude numbers in the non-planing region with Froude number in the range  $0.2 < Fr < 0.7$ . At higher Froude numbers, the force generated by the vane creates an unbeneficial bow-down trim as observed experimentally during the towing tests and using CFD simulations. Considering also a crew boat as in this study, an increase of ship resistance

was reported at Froude numbers  $Fr < 0.45$  when a Hull Vane<sup>®</sup> was applied [10-11]. Therefore, the recommended Froude number range for an application of a Hull Vane<sup>®</sup> is  $0.5 < Fr < 0.7$  for this type of ship.

Figures 8 and 9 show a comparison of visualizations obtained from the CFD simulations and the towing tests ( $Fr = 0.62$ ). Both the CFD and experimental results show a local high overflow of water near the bow. This locally high water-overflow near the bow is ascribed partly to the hard chine body. As shown in Figure 8 (right panels), a bow-down trim was observed due to the application of the Hull Vane<sup>®</sup> which becomes more pronounced with increasing  $Fr$ . This observation is consistent with the prediction, as also reported in Ref. [3]. As noted earlier, Case 3 shows a decrease in ship resistance and the bow-down trim for this case is the smallest compared to the Cases 1 and 2. Furthermore, Figure 9 shows that the wave patterns obtained from the CFD simulations agree well with those obtained from the experiments.



**Fig. 8.** Comparison of visualizations of water surface elevations near the bow and near the stern obtained from CFD simulations and towing tests ( $Fr = 0.62$ ); (a) Case 0, (b) Case 1, (c) Case 2 and (d) Case 3



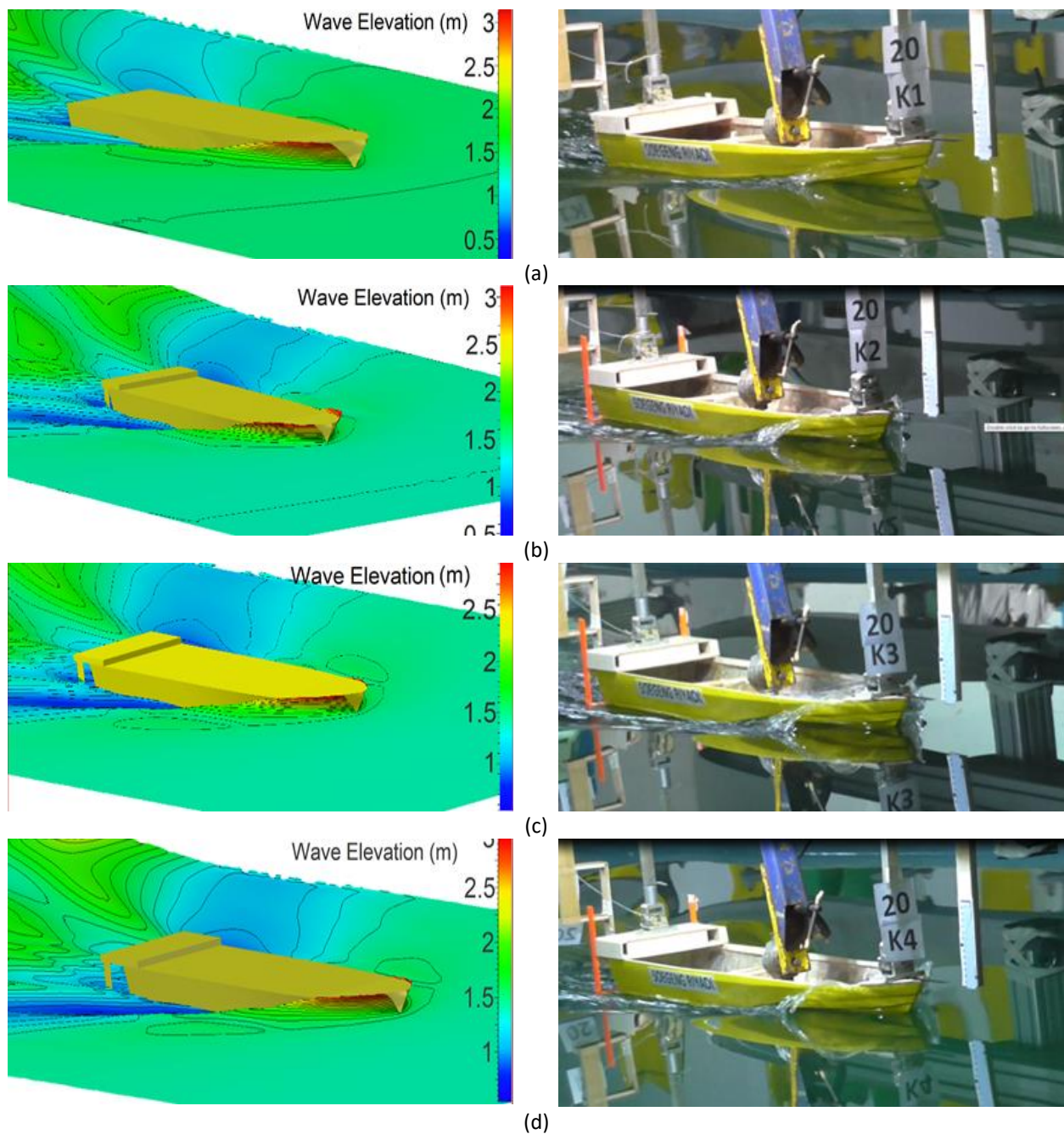


**Fig. 9.** Comparison of visualizations of 3-D wave pattern obtained from CFD simulations and towing tests ( $Fr = 0.62$ ); (a) Case 0, (b) Case 1, (c) Case 2 and (d) Case 3

Figure 10 shows that the wave pattern behind the vessel is changed slightly and the wave height is reduced due to the application of the Hull Vane<sup>®</sup>. The generated waves have higher crests for the case without vane as shown in Figure 10(a) (approximately 2.5 m), compared to those for the cases with vane (Figure10(b-d), approximately 1.5 m).

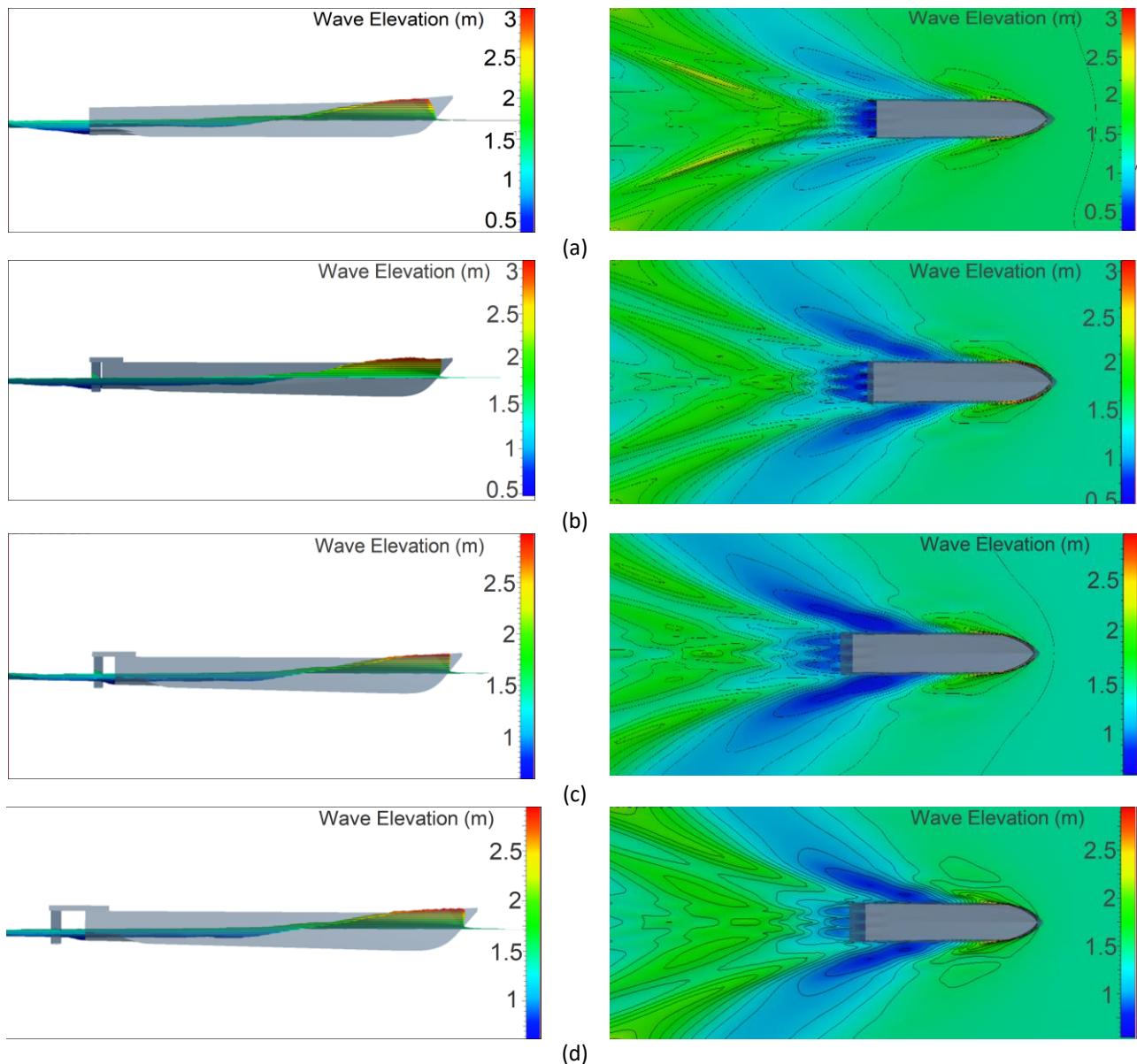


**Fig. 10.** Wave elevation and wave pattern obtained from the CFD simulations ( $Fr = 0.62$ ); (a) Case 0, (b) Case 1, (c) Case 2 and (d) Case 3

#### 4. Conclusions

To investigate the possibilities of energy efficiency when a Hull Vane<sup>®</sup> is to be retrofitted into a high speed craft at  $Fr > 0.6$ , CFD simulations and towing-tank experiments were performed in which the vane's placement was varied in the longitudinal direction but its submerged elevation was kept constant at  $0.75 T$  below the water surface, where  $T$  is the boat's draft. Three variations of vane's placement in the longitudinal directions were considered: (i) vane's leading edge in-line with the transom (Case 1), (ii) vane's leading edge one chord length behind the transom (Case 2) and (iii) vane's leading edge two chord lengths behind the transom (Case 3). A 31 m hard-chine crew boat was considered, which was designed and produced by PT. Orela Shipyard, Gresik Indonesia.

At  $Fr > 0.75$  all vane's placements resulted in an increase of the total ship resistance, reaching a value of 36.3% for Case 2 at  $Fr = 0.92$ . A bow-down trim was observed, which became more pronounced with increasing  $Fr$ . From the cases considered, the vane's position with the leading edge two chord lengths behind the transom (Case 3) gave the smallest ship resistance. At  $Fr < 0.74$ , this

vane positioning resulted in a decrease of ship resistance, which reached 7.1% at  $Fr = 0.62$ . Referring to the results of previous studies [10-11] in addition to the present results, the recommended Froude number range for Hull Vane®'s applications for this type of ship is  $0.5 < Fr < 0.7$ .

The CFD successfully simulates the physical phenomena observed during the towing tests, such as the wave patterns and the locally high water-overflow near the bow. The application of the Hull Vane® reduces the height of the waves generated by the ship.

## Acknowledgements

This research project was supported by the Ministry of Research, Technology and Higher Education of the Republic of Indonesia and PT. Orela Shipyard, Gresik, Indonesia, under the grant Penelitian Terapan Unggulan Perguruan Tinggi (Penelitian Kerjasama Industri) with contract no. 1031/PKS/ITS/2018.

## References

- [1] Marine Environment Protection Committee. "Guidelines on the method of calculation of the attained energy efficiency design index (EEDI) for new ships." *Resolution MEPC 212* (2012): 63.
- [2] MEPC, RESOLUTION. "2016 GUIDELINES FOR THE DEVELOPMENT OF A SHIP ENERGY EFFICIENCY MANAGEMENT PLAN (SEEMP)." *International Maritime Organization. London 2* (2012).
- [3] Uithof, K., P. van Oossanen, N. Moerke, P. G. van Oossanen, and K. S. Zaaier. "An update on the development of the Hull Vane." In *9th International Conference on High-Performance Marine Vehicles (HIPER), Athens*. 2014.
- [4] Bouckaert, B., K. Uithof, P. G. Van Oossanen, and N. Moerke. "Hull Vane on Holland-Class OPVs—A CFD Analysis of the Effects on Seakeeping." In *13th International Naval Engineering Conference and Exhibition (INEC), Bristol*. 2016.
- [5] Bouckaert, B., K. Uithof, PG van Oossanen, N. Moerke, B. Nienhuis, and J. van Bergen. "A life-cycle cost analysis of the application of a Hull Vane to an Offshore Patrol Vessel." In *13th International Conference on Fast Sea Transport (FAST), Washington DC*. 2015.
- [6] Uithof, K., B. Bouckaert, P. G. van Oossanen, and N. Moerke. "The Effects of the Hull Vane® on Ship Motions of Ferries and RoPax Vessels." *RINA Design & Operation of Ferries & Ro-Pax Vessels, London* (2016).
- [7] Uithof, K., N. Hagemester, B. Bouckaert, P. G. van Oossanen, and N. Moerke. "A systematic comparison of the influence of the Hull Vane®, interceptors, trim wedges, and ballasting on the performance of the 50m AMECRC series# 13 patrol vessel." *Proc. Warship* (2016).
- [8] Suastika, Ketut, Bonaventura D. Prasetyo, Marshall Boazyunus, I Ketut Aria Pria Utama, and Soegeng Riyadi. "Hull-Vane® Submerged-elevation Optimization for Improved Seakeeping Performance: A Case Study of an Orela Crew Boat." In *Proceeding of Marine Safety and Maritime Installation* p. 349-357, Bali, Indonesia. 2018.
- [9] Suastika, Ketut, Affan Hidayat, and Soegeng Riyadi. "Effects of the application of a stern foil on ship resistance: A case study of an Orela crew boat." *Int. J. Tech* 8, no. 7 (2017): 1266-1275.
- [10] Suastika, I.K., A. Firdhaus, R. Akbar, W.D. Aryawan, I.K.A.P. Utama, S. Riyadi, and B. Ganapathisubramani. "Experimental and Numerical Study of Ship Resistance due to Variation of Hull Vane® Positioning in the Longitudinal Direction," In *Proceedings of International Conference on Ship and Offshore Technology* (2019), Semarang, Indonesia.
- [11] Abbott, Ira H., and Albert E. Von Doenhoff. *Theory of wing sections: including a summary of airfoil data*. Courier Corporation, 2012.
- [12] FINE/MARINE®. *User Manual: Flow Integrated Environment for Marine Hydrodynamics*. Belgium: Numeca International, 2013.
- [13] Versteeg, Henk Kaarle, and Weeratunge Malalasekera. *An introduction to computational fluid dynamics: the finite volume method*. Pearson education, 2007.
- [14] Menter, Florian R. "Two-equation eddy-viscosity turbulence models for engineering applications." *AIAA journal* 32, no. 8 (1994): 1598-1605.
- [15] ISIS-CFD v3.1. *Theoretical Manual*. EMN, Ecole Centrale de Nantes, France, 2013.
- [16] Hirt, Cyril W., and Billy D. Nichols. "Volume of fluid (VOF) method for the dynamics of free boundaries." *Journal of computational physics* 39, no. 1 (1981): 201-225.
- [17] Ali, Arifah, Adi Maimun, and Yasser Mohamed Ahmed. "Analysis of Resistance and Generated Wave around Semi SWATH Hull at Deep and Shallow Water." *Journal of Advanced Research in Fluid Mechanics and Thermal Sciences* 58, no. 1 (2019): 247-260.
- [18] Anderson, John David, and J. Wendt. *Computational fluid dynamics*. Vol. 206. New York: McGraw-Hill, 1995.